AAPS PharmSciTech, Vol. 11, No. 1, March 2010 (© 2010)
DOI: 10.1208/s12249-010-9393-0

Research Article

Chitosan and Glyceryl Monooleate Nanostructures Containing Gemcitabine: Potential Delivery System for Pancreatic Cancer Treatment

William J. Trickler,[1] Jatin Khurana,[1] Ankita A. Nagvekar,[1] and Alekha K. Dash[1,2]

Received 23 June 2009; accepted 16 February 2010; published online 18 March 2010

Abstract. The objectives of this study are to enhance cellular accumulation of gemcitabine with chitosan/glyceryl monooleate (GMO) nanostructures, and to provide significant increase in cell death of human pancreatic cancer cells *in vitro*. The delivery system was prepared by a multiple emulsion solvent evaporation method. The nanostructure topography, size, and surface charge were determined by atomic force microscopy (AFM), and a zetameter. The cellular accumulation, cellular internalization and cytotoxicity of the nanostructures were evaluated by HPLC, confocal microscopy, or MTT assay in Mia PaCa-2 and BxPC-3 cells. The average particle diameter for 2% and 4% (*w*/*w*) drug loaded delivery system were 382.3±28.6 nm, and 385.2±16.1 nm, respectively with a surface charge of +21.94±4.37 and +21.23±1.46 mV. The MTT cytotoxicity dose-response studies revealed the placebo at/or below 1 mg/ml has no effect on MIA PaCa-2 or BxPC-3 cells. The delivery system demonstrated a significant decrease in the IC50 (3 to 4 log unit shift) in cell survival for gemcitabine nanostructures at 72 and 96 h post-treatment when compared with a solution of gemcitabine alone. The nanostructure reported here can be resuspended in an aqueous medium that demonstrate increased effective treatment compared with gemcitabine treatment alone in an *in vitro* model of human pancreatic cancer. The drug delivery system demonstrates capability to entrap both hydrophilic and hydrophobic compounds to potentially provide an effective treatment option in human pancreatic cancer.

KEY WORDS: chitosan; gemcitabine; glyceryl monooleate; nanostructure; pancreatic cancer.

INTRODUCTION

Annually 33,000 and 60,000 people are diagnosed with malignant tumor growth in the pancreatic gland in the USA and Europe. With 32,180 new diagnoses in the USA every year, and 31,800 deaths, mortality approaches 99%, giving pancreatic cancer the highest fatality rate of all cancers and the fourth highest cancer killer in the USA among both men and women (1,2). By the time pancreatic cancer is diagnosed, most people already have disease that has spread to distant sites in the body and the median survival time is around 3 to 6 months; 5-year survival is much less than 5% with few victims still surviving 5 years after diagnosis, and complete remission still extremely rare (1,2). The statistical incidence and patient prognosis reflect significant challenges in the treatment of pancreatic cancer, and the relative deficiencies in treatment options.

Currently, the treatment options are limited to localized resection of pancreatic tumors and chemotherapy. Chemotherapeutic agents of choice are 5-fluorouracil, gemcitabine, and erlotinib. Although these chemotherapeutics have direct effects on cancerous tissues, the toxicities in normal tissues are usually dose-limiting factors in successful chemotherapeutic regimes. Gemcitabine has been approved by the FDA for use as a single agent for the first line treatment of both locally advanced and metastatic cases of pancreatic cancer (3–5). Gemcitabine is a difluoro analog of deoxycytidine and has a dual mechanism of action. It is transported into cells by nucleoside transporters, where it is phosphorylated to difluoro deoxycytidine diphosphate (dfdCDP) and triphosphate (dfdCTP). The diphosphate (dfdCDP) is a ribonucleotide reductase inhibitor and thus diminishes the availability of deoxyribonucleotides essential for DNA synthesis, whereas the triphosphate analog (dfdCTP) competes with cytidine triphosphate to get incorporated in the DNA and leads to DNA strand termination (6). The dual mechanism of action of gemciatbine makes it a very potent chemotherapeutic agent for the treatment of adenocarcinomas. However, the major setbacks to the current clinical treatment with gemcitabine include its short half-life and low permeability. Gemcitabine is rapidly metabolized in plasma into difluorodeoxyuridine (dfdU) by the enzyme cytidine deaminase (4). The plasma half-life of gemcitabine following intravenous infusion is 8–17 min in human plasma and 9 min in murine plasma (7–9). Therefore, it requires administration of high doses leading to dose-limiting adverse effects. Also, gemcitabine is a very hydrophilic molecule with a log(*P*) value of −1.4 and requires assistance of nucleoside transporters to reach the intracellular site of action (10,11). A deficiency of these transporters is the most common mechanism for development

[1] Department of Pharmacy Sciences, School of Pharmacy and Health Professions, Creighton University Medical Center, 2500 California Plaza, Omaha, Nebraska 68178, USA.
[2] To whom correspondence should be addressed. (e-mail: adash@creighton.edu)

of resistance to gemcitbaine (10,12). These limiting factors provide compelling evidence that the development of new approaches to deliver chemotherapeutics becomes imperative. Recent trends to overcome these obstacles have been in the areas of targeted or localized delivery. Different polymeric systems have been used for incorporating gemcitabine which include poly ε-caprolactone (13), polyethylcyanoacrylate (14). Nanoparticle based delivery system using Cetuximab as a targeting agent has been developed and tested in the treatment of pancreatic cancer (15). Gang and coworkers have shown the effectiveness of magnetic poly epsilon-caprolactone nanostructure-containing ferric oxide and gemcitabine in the treatment of pancreatic cancer in pancreatic cancer xenografts mouse model (16). Stella and coworkers evaluated the use of polycyanoacrylate to fabricate nanoparticles for a lipophilic conjugate of gemcitabine. The gemcitabine conjugate was synthesized by covalently linking an acyl chain to the 4-amino group on the gemcitbine (17). Nanoparticles of gemcitabine were also prepared by covalently linking gemcitabine with 1,1′,2-tris-nor-squalenic acid. These nanoparticles exhibited higher toxicity in murine-resistant leukemia and human-resistant leukemia cell lines (18). Gemcitabine nano-particles have also been produced by entrapping the drug in polybutylcyanoacrylate (19). Polymeric nanogels of gemcitabine encapsulated in biodegradable polymers consisting of polyethylene glycol and polyethylene imine crosslinked via disulfide bonds has been developed and tested for efficacy in breast and colorectal cancers (20). Arias and group have also evaluated the cytotoxicity of gemcitabine loaded polybutylcyanoacrylate nanoparticles in murine leukemia cells (21). Gemcitabine nanoparticles formulated using bovine serum albumin, were found to significantly improve its anti-proliferative activity, when tested on human pancreatic cancer lines (BxPc-3) (22).

By definition, a targeted or localized delivery selectively transports an agent for a characteristic effect to the site of action. One of the various methods to achieve this is through bioadhesive delivery systems formulated to enhance drug bioavailability by adherence with the mucosal surface associated with epithelial cellular surfaces. Chitosan has been shown to have certain bioadhesive properties due to interactions with the mucosal membranes associated with epithelial barriers and tumors (23–26). Glyceryl monooleate (GMO) has been reported to form liquid crystals in water through phase transformations (27). The cubic phase formed in water is a three dimensional network of curved lipid bilayers separated by an intricate network of water channels (27,28). Our lab previously demonstrated mucoadhesive properties of an *in situ* gel consisting of chitosan/GMO for the delivery of paclitaxel (PTX) (29,30). However, the precise mechanistic interactions between chitosan and the mucosal barriers or the glycosylation sites on tumors remain unclear. More recently, our laboratory has been involved with the same bio-materials to develop nanostructures for the delivery of both hydrophilic and hydrophobic compounds. The *in vitro* sub-cellular localization and *in vivo* efficacy of chitosan/GMO nanostructures containing hydrophobic compounds like PTX has already been documented (29,31). These nanostructures obtained after lyophilization were easily redispersed in water for injection and were administered via parenteral routes. We have previously shown that chitosan/GMO can also sustain the release of paclitaxel (32). We hypothesize that a bioadhesive, sustained release formulation would improve the cellular accumulation and cytotoxicity of gemcitabine in human pancreatic cancer cell lines. The current report further describes lyophilized chitosan/GMO nanostructures to increase the therapeutic efficacy of gemcitabine in epithelial cells derived from cancerous pancreatic tissues. We also envisage a similar route of administration for gemciabine nanostructures as used in case of PTX. BxPC-3 and Mia PaCa-2 cell monolayers were selected as *in vitro* cellular models to identify the cytotoxicity of gemcitabine loaded delivery system using MTT assay. BxPC-3 and Mia PaCa-2 are known to produce mucin (33,34). We have previously reported the cellular association of chitosan/GMO particles in mucin producing CaCo-2 and Calu-3 cell lines (32). The subcellular association of the delivery system in BxPc-3 and Mia PaCa-2 cell monolayers was studied via confocal microscopy using nanostructures loaded with coumarin.

MATERIALS AND METHODS

Materials

Gemcitabine (Gemzar™) was purchased from Creighton University Medical Center Pharmacy (Omaha, NE). BxPC-3 and Mia PaCa-2 pancreatic cancer cell lines were purchased from American Type Culture Collection (Manassas, VA). The Gibco brand cell culture media and constituents, RPMI 1640, Dulbecco's modified Eagle medium (DMEM), fetal bovine serum (FBS), penicillin/streptomycin, trypsin-EDTA, L-glutamine, sodium pyruvate, and non-essential amino acids were purchased from Invitrogen (Carlsbad, CA). GMO was obtained from Eastman Chemical Company (Kingsport, TN). Anhydrous citric acid was purchased from Acros Organics (Fairlawn, NJ). Acetonitrile (high-performance liquid chromatography (HPLC)), ammonium acetate (HPLC), sodium phosphate monobasic, sodium phosphate dibasic, hydrochloric acid (reagent grade), Triton-X-100, and Falcon™ tissue culture flasks and Falcon™ tissue culture plates were purchased from Fisher Scientific (Fairlawn, NJ). Sodium chloride and coumarin-6 (fluorescent laser dye) was purchased from Sigma Chemical Company (St. Louis, MO). Low molecular weight chitosan (<6,000) with a brookfield viscosity of 20.0 cps was purchased from Aldrich Chemical Company (Milwaukee, WI).

Formulation Preparation

The formulation was prepared by a multiple emulsion followed by solvent evaporation as previously described (29). Briefly, Gemzar™ is a commercially available injectable formulation when reconstituted as directed in sterile water the concentration of gemcitabine is 38 mg/ml. GMO is a semisolid at room temp and melts at 40°C producing a fluid phase. Gemcitabine (38 mg/ml stock; 1 ml for 2%) or (2 ml for 4%) was incorporated into the fluid phase of GMO (1.75 ml at 40°C) (*w/o*) to form a primary emulsion. This primary emulsion was further mixed with 12.5 ml of polyvinyl alcohol dissolved in sterile deionized water (0.5% *w/v*; mw 30,000–70,000) by ultrasonication (18 watts for 2 min; Soni-

cator 3000, Misonix, Farmingdale, NY). Finally the secondary emulsion was prepared by mixing the primary emulsion described earlier with a chitosan solution (12.5 ml; 2.4% *w*/*v*) dissolved in citric acid (100 mM) by ultrasonication (18 watts for 2 min). From our previous studies, it was evident that in order to achieve smaller particle size as well as easily redispersible nanoparticles of chitosan/GMO, low molecular weight chitosan was required (29). Therefore, low molecular weight chitosan was used in this entire study. The multiple emulsion formed (*w*/*o*/*w*) was frozen (−80°C) prior to solvent evaporation by freeze drying method (−52°C and<0.056 mBar pressure; FreeZone, Labconco, St Louis, MO).

Characterization

The nanostructure size and zeta potential were determined using a zetameter (ZetaPlus, Brookhaven Instruments Corporation, Holtsville, NY). The lyophilized nanostructures were resuspended in deionized water (0.4 mg/ml) for particle size and zetapotential analysis. For the atomic force microscopy (AFM) studies, the nanostructures (10 mg) were resuspended in deionized water (1 ml). Sample droplets (10 μl) were deposited on bare-mica and dried under an argon matrix. The bare-mica was attached to a metal disc with double-stick tape for imaging. Images were acquired in air and using a Multimode SPM Nanoscope IV system (Veeco/Digital Instruments, Santa Barbara, CA). Silicon-etched tapping mode probes were used (TESP7; Veeco/Digital Instruments, Santa Barbara, CA). The acquired images are representative of two different batches of nanostructures.

The HPLC separation of gemcitabine was attained with a C18 Luna column (250×4.6 mm, 5 μm; Phenomenex, Torrance, CA). The stationary phase was perfused with a mobile phase (95/5% (*v*/*v*), 40 mM ammonium acetate: acetonitrile, pH5.5) at a flow rate of 1.0 ml/min at ambient temperature. The effluents were monitored at 268 nm and quantified using the area under the peak from standard solutions dissolved in mobile phase (0.4 to 20 μg/ml; Shimadzu SP-10A VP, Columbia, MD).

The *in vitro* drug release profile from the formulation was determined by measuring the cumulative amount of drug released from the nanoparticle over a predetermined experimental period (1 to 48 h). Briefly, the formulation (2 mg) was dispersed in 40 ml of PBS (pH7.4) in a capped Erlenmeyer flask in triplicate and agitated in a water bath (37°C and 80 rpm). An HPLC sample was removed (200 μl) with a filter tip needle at various time intervals and replaced with fresh media. The total amount of drug present was determined in separate studies. Briefly, the formulation (2 mg) was dispersed in 15 ml of acetonitrile/water (60:40 *v*/*v*) and sonicated (Fisher Scientific FS 20, Fairlawn, NJ) for 4 h to extract the drug from the nanostructure. The extracted solution was filtered, diluted with the mobile phase and the drug content was determined by HPLC. In addition, the percent drug load was calculated by taking the ratio of drug extracted to the total weight of the formulation containing the drug. Since no washing step was included while formulating the nanostructures, one should expect no loss of entrapped as well as free drug during this preparation. Therefore the yield is expected to be 100% and the true entrapment efficiency of the nanoparticles was difficult to determine.

The Cellular Association of Chitosan/GMO

The cellular accumulation of gemcitabine was evaluated in human pancreatic cancer cells BxPC-3 and Mia PaCa-2 cells previously described (29). Briefly, the cells were cultured in standard Falcon™12-well tissue culture plates at a seeding density of 200,000 cells per square centimeter and cultured until confluency in a humidified chamber at 37°C in Roswell Park Memorial Institute (RPMI-1640) medium (BxPC-3 cells) or DMEM (Mia PaCa-2 cells) growth media supplemented with 10% FBS, 1% L-glutamine, 1% sodium pyruvate, 1% non-essential amino acids, and 1% penicillin/streptomycin. Confluent cell monolayers were treated with a single bolus solution of gemcitabine (1 μM) or the nanostructures loaded with equivalent gemcitabine in assay II buffer for various times (30 or 60 min). The cell monolayers were washed three times with ice cold PBS and lysed with triton-X-100 (1% *v*/*v*). The cell lysates were collected in a microcentrifuge tube and a sample (25 μl) was assayed for total protein content by the bicinchoninic acid protein assay (Pierce, Rockford, IL). The microcentrifuge tubes were centrifuged at 14,000 rpm in a microcentrifuge for 30 min at 4°C (accuSpin Micro R, Fisher Scientific, Fairlawn, NJ). The amount of gemcitabine in the supernatant was determined and quantified by HPLC methods as previously described. A sample of the dose (1 ml) for each group was frozen (−80°C) prior to solvent evaporation by freeze drying (−52°C and <0.056 mBar pressure) (FreeZone, Labconco, Kansas City, MO). The freeze dried dose samples were resuspended in 1% triton-X-100, agitated at 100 rpm for 30 min at 37°C in an incubated shaker (Orbit, Labline Instruments Inc., Melrose Park, IL), and the amount was determined by HPLC. To control for any dosing variations, the percent accumulation was calculated as a ratio of the amount of cellular accumulated gemcitabine divided by the total gemcitabine dose normalized to total cellular protein from the separate cell monolayers.

The Cytotoxicity Profile of Chitosan/GMO Nanostructures

MTT cytotoxicity analysis was used to determine the viability of human pancreatic cancer cells following exposure to various chitosan/GMO nanostructures. Briefly, the cells were seeded in a 96-well cell culture plate at a density of 10,000 cells per well and incubated overnight in a humidified chamber at 37°C in the appropriate growth medium RPMI-1640 (BxPC-3 cells) or DMEM (Mia PaCa-2 cells) supplemented with 10% FBS, 1% L-glutamine, 1% sodium pyruvate, 1% non-essential amino acids, and 1% penicillin/streptomycin. The cells were treated with various concentrations (10^{-7} to 10^{-1}M) in a single bolus with a solution of gemcitabine or nanostructures containing equivalent amounts of gemcitabine or equivalent amounts of blank nanostructures suspended in sterile water for 4 h, then washed three times with PBS and supplied with fresh growth media (72-to-96 h). After the incubation period, the cells were treated with fresh MTT reagent (25 μL, 5 mg/ml) and further incubated for 4-h, then treated with a fresh solvent (100 μL) consisting of 20% (*w*/*v*) sodium dodecylsulfate dissolved in water at 37°C mixed with an equal volume of DMF (dimethyl formamide). The solvent pH was adjusted to 7.4 using 2.5% of 80% acetic acid and 1% of 1N HCl. The

absorbance was read on a microplate reader at 550 nm. The absorbance data was analyzed and presented as percent survival of control monolayers receiving media alone.

Chitosan/GMO Nanostructure Sub-Cellular Localization by Confocal Microscopy

The *in vitro* cellular association and sub-cellular localization of the delivery systems were evaluated in BxPC-3 and Mia PaCa-2 human pancreatic cancer cell lines. In these studies, cells were cultured on Falcon multiwell slides. Briefly, the cells were seeded in a multiwell cell culture slide at a density of 10,000 cells per well and incubated overnight in a humidified chamber at 37°C in the appropriate growth medium supplemented as previously described. The cells were treated with the either chitosan/GMO nanostructures loaded with coumarin-6 (fluorescent laser dye) as a function of time (30 or 60 min) in assay buffer spiked with lysotracker red (50 nM). The adherent cells were washed three times in ice cold PBS and fixed with para-formaldehyde (4%). The wells were removed and the cells were further stained with mounting media consisting of DAPI (1.5 μg/ml), *n*-propyl gallate (0.1 g) in PBS buffered glycerol and sealed with coverslips. The slides were viewed on a multi-photon confocal microscope (Carl Ziess, Germany) at the Nebraska Center for Cell Biology at Creighton University.

Statistical Analyses

The results are expressed as mean±standard error of the mean for all quantitative data. The quantitative data was statistically analyzed using single factor analysis of variance followed by Tukey's multiple post-hoc test for paired comparisons of means (SPSS 10, SPSS Inc., Chicago, IL). For all studies, statistical significance was designated as $p<0.05$, unless otherwise stated.

RESULTS

Nanoparticle Characterization

The size and surface charge characteristics of chitosan/GMO nanostructures with or without gemcitabine are summarized in Table I. The mean particle size ranged from 382 nm (gemcitabine) to 436 nm (coumarin-6), and the surface charge ranged from 21 mV (gemcitabine) to 32 mV (coumarin-6). The drug load and the hydrophobicity of the drug molecule involved had no statistically significant effect on the particle size (p value >0.05). However, the incorporation of gemcitabine decreased the surface charge by approximately 10 mV. The AFM images show approximately spherical structures (Fig. 1) within the size range summarized in Table I. In addition, the micrographs show a distribution of various nanostructure sizes.

The release of gemcitabine from nanostructures was determined by measuring the cumulative amount of drug released over various time intervals (0–48 h) (Fig. 2). The *in vitro* gemcitabine release profile showed common characteristics of burst release initially followed by a slow rate of release with a maximal of 40% gemcitabine released in 48 h.

The Cellular Accumulation of Chitosan/GMO Nanostructure

The cellular accumulation of gemcitabine was quantitatively determined by HPLC methods in Mia PaCa-2 or BxPC-3 cells (Fig. 3). The cellular accumulation of gemcitabine was significantly higher with the chitosan/GMO nanostructures when compared with a solution of gemcitabine throughout the entire study period in both cell lines. The percent accumulated dose was approximately 2-fold higher when compared with a solution of gemcitabine throughout the entire experimental period. The over-all magnitude of accumulated gemcitabine in BXPC-3 cells was significantly higher when compared with the Mia PaCa-2 cells.

The Cytotoxicity Profile of Chitosan/GMO Nanostructure

The viability of human pancreatic cancer cells was determined using MTT cytotoxicity analysis (Figs. 4 and 5). The dose-response studies demonstrated that chitosan/GMO nanostructures without gemcitabine have little effect on the cell viability in these two human pancreatic cancer cells (Figs. 4 and 5). The dose-response studies further showed that either Mia PaCa-2 (Fig. 4) or BxPC-3 (Fig. 5) cells exposed to an equivalent dose of gemcitabine loaded nanostructures for 4 h had significantly increased cell death when compared with the solution alone at both (A) 72-h and (B) 96-h post-treatment (Figs. 4 and 5). The fold decrease in IC50 was approximately 3- to 4-fold at 72 and 96 h post-treatment when compared with gemcitabine solution (conventional therapy) alone (Table II).

Chitosan/GMO Nanoparticle Sub-Cellular Localization by Confocal Microscopy

The *in vitro* cellular association and sub-cellular localization of the delivery systems were evaluated in both Mia PaCa-2 or BxPC-3 cells human pancreatic cancer cells by confocal microscopy methods (Fig. 6). In both cell lines, the fluorescent NPs appear to be qualitatively internalized in a

Table I. Chitosan/GMO Nanostructure Characteristics

Nanostructure type	Particle size (nm) mean±SEM, $n=3$	Particle charge (mV) mean±SEM, $n=3$
Blank chitosan/GMO	432.0±16.3	+31.78±0.54
2% (*w*/*w*) gemcitabine chitosan/GMO	382.3±28.6	+21.94±4.37
4% (*w*/*w*) gemcitabine chitosan/GMO	385.2±16.1	+21.23±1.46
0.1% (*w*/*w*) coumarin-6 chitosan/GMO	436.5±4.9	+32.1±6.15

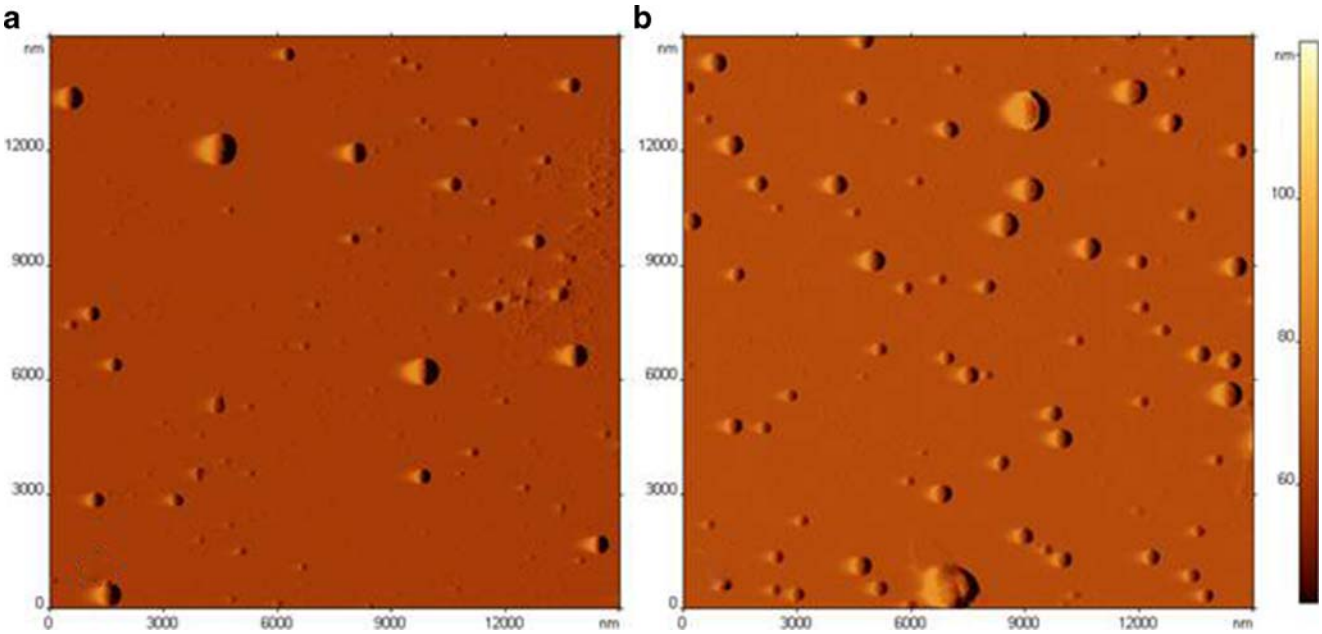

Fig. 1. Atomic force microscopic images of chitosan/GMO nanostructures in the absence of GEM (**a**) and the presence of GEM (**b**)

time dependent manner. Both Mia PaCa-2 cells and BxPC-3 cells were also evaluated in the absence of nanostructures and with an equivalent (free fraction of coumarin-6) solution with no fluorescence observed (data not shown). In addition, the internalization of the nanostructures appears to be an endo-lysosomal mechanism by the co-localization of green fluorescent dye with the lysotracker red dye. Furthermore, the lack of co-localized green fluorescent dye with the blue fluorescent dye indicates no co-localization within the nuclear compartment in these cell types.

DISCUSSION

Our laboratory has previously been involved in the development of nanostructures for localized delivery of chemotherapeutics and potentially to passively target cancerous tissues through the synergistic bioadhesive properties of both chitosan and GMO. However, we have only reported chitosan/GMO nanostructures for the delivery of hydrophobic compounds like PTX (29). The current report further describes lyophilized chitosan/GMO nanostructures to increase the therapeutic efficacy of hydrophilic compounds like gemcitabine in epithelial cells derived from cancerous pancreatic tissues. Previous studies characterized the physicochemical properties and demonstrated an increased efficacy of paclitaxel due to the increased cellular association of paclitaxel with chitosan/GMO nanostructures in human breast cancer cells (MDA-MB-231). In addition, the increased cellular association of paclitaxel was attributed to the bioadhesive nature of both chitosan and GMO (29). The synergistic adhesive properties of chitosan/GMO have been reported elsewhere (30,32). In these studies, the authors reported increased mucin adhesion with both chitosan and GMO compared with either alone by the shear force measurements (30,32). Others have reported mucin adhesion of chitosan coated liposome to the intestinal mucosal both *in vitro* and *in vivo* (24,35–38). In addition, reports have shown the adhesive nature of chitosan nanostructure and coated liposome to the aberrant glycosylation sites associated with cancerous cells both *in vitro* and *in vivo* (24,37–40). Studies by Shikata *et al.* (2002), demonstrated increased cellular internalization of chitosan nanostructure in various cancerous cells compared with solutions alone (40). The exact cellular adhesive mechanisms for the interactions with chitosan remain unclear. However, together, these studies provide compelling evidence that chitosan may passively target cellular tissues that over-produce mucins.

Nanoparticle Characterization

The entrapment of gemcitabine in the chitosan/GMO nanostructures showed no statistical change in the approximate 400 nm size of the nanostructures. In contrast to previous studies with paclitaxel, that demonstrated a decreasing size with increasing hydrophobicity of the entrapped compound. The difference in the methodology used in the structural formation can possibly account for the slightly

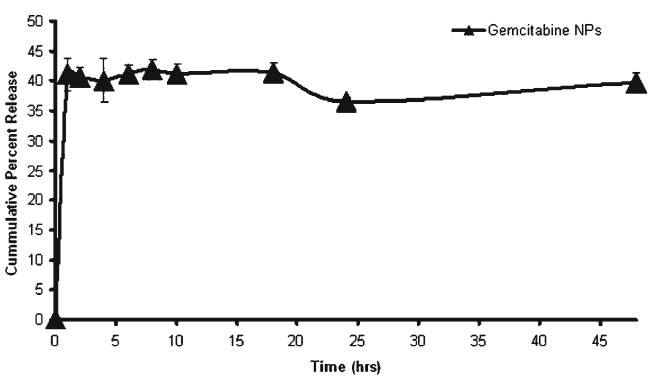

Fig. 2. *In vitro* release of GEM from Chitosan/GMO nanoparticles

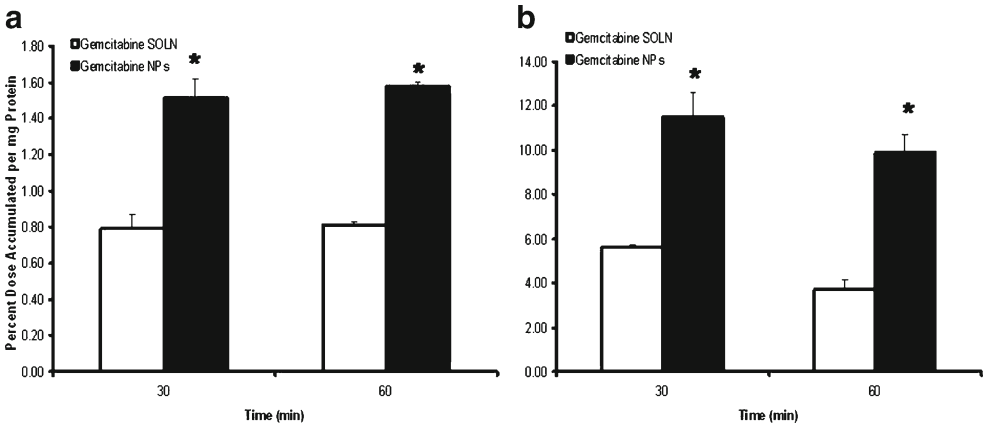

Fig. 3. Accumulated dose of gemcitabine in **a** Mia PaCa-2 cells and **b** BxPC-3 Cells. The data is expressed as mean±SEM from three separate experiments ($n=3$). *$p<0.05$, statistically significant when compared with GEM solution alone. (Note 10-fold difference in y abscissa)

smaller size. In the current studies, aqueous solution of gemcitabine was incorporated into the GMO as an (*w/o*) emulsion as opposed to the direct entrapment of crystalline paclitaxel, dexamethasone, and coumarin-6 to the molten GMO described in our earlier report (29). Previously, we examined the micromorphology of chitosan/GMO nanostructures to be smooth non-porous individual particles with round to elliptical shape (29). In agreement with those studies, the AFM images reported here further confirm the structural micromorphology to be smooth individual spherical structures with a varying size distribution. In agreement with these observations, others have observed similar findings with chitosan-modified lipid-based systems (25,35,37,38,41). The highly positive surface charge of the nanostructures provides compelling evidence that the protonated amino groups of chitosan are structurally oriented on the surface of the chitosan/GMO nanostructures, and GMO forms a central core. The transmission electron microscopic studies of these chitosan/GMO nanostructures with osmium tetraoxide have clearly shown the presence of a hydrophobic inner core formed of GMO surrounded by a hydrophilic surface layer consisting of chitosan (29)**.** This structural orientation of the nanostructures can explain release pattern characteristics and alterations in surface charge.

In Vitro Release

The characteristic burst release observed with nanostructures consisting of chitosan/GMO can obviously be explained by surface bound or free drug. In the current study, differences in nanostructure surface charge possibly indicate surface bound interactions between the protonated amino groups of chitosan and gemcitabine. The positive surface charge on chitosan/GMO particles could result from preferential adsorption and/or by ionization. The Table I depicts the zeta potential of the blank particles (~32 mV) as compared with particles containing 4% gemcitabine (~21 mV). This significant decrease in zeta potential could potentially be explained by both preferential adsorption of gemcitbaine on to the surface of chitosan and by ionization. Gemcitbaine hydrochloride is a salt of weak base (gemcitbaine) and strong acid (hydrochloric acid), the ionization of the amine residues of chitosan molecules is expected to be hindered by the presence of gemcitbaine hydrochloride (pKa 3.6) in an environment that is acidic in nature. However, these interactions would still be considered free drug. Secondly, structural boundary layers can provide a plausible explanation for limited terminal release of gemcitabine from the nanostructures; the diffusional barriers for the release of the

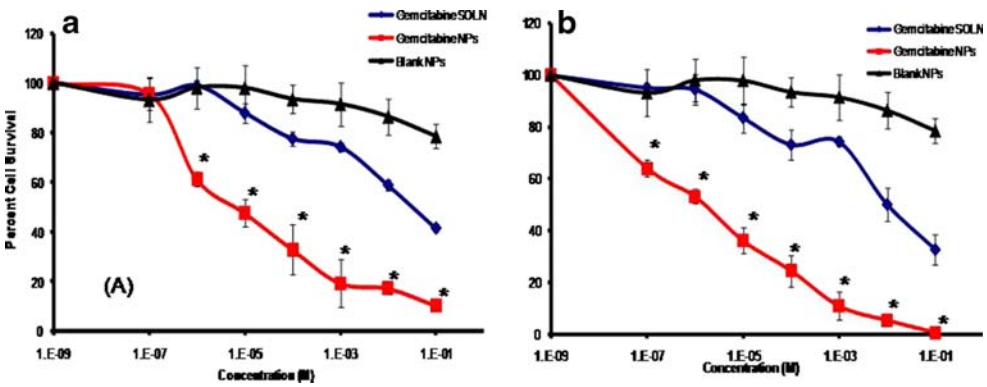

Fig. 4. The cytotoxicity effects of GEM **a** 72 h post-treatment and **b** 96 h post-treatment in Mia PaCa-2 Cells. The data is expressed as mean±SEM from three separate experiments in triplicate ($n=9$). *$p<0.05$, statistically significant inhibitory effect when compared with gemcitabine solution alone

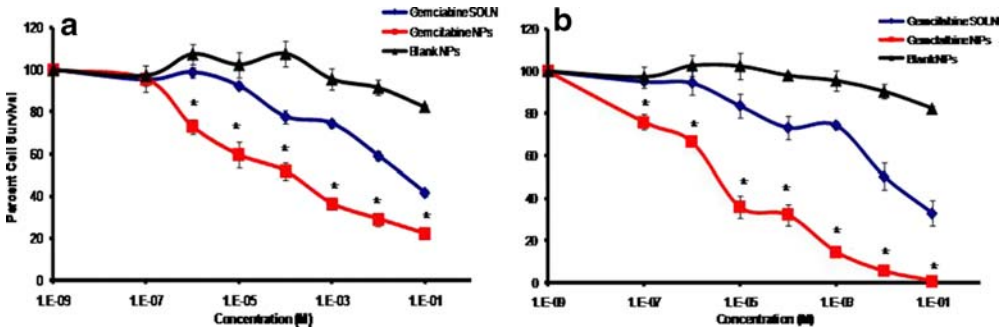

Fig. 5. The Cytotoxicity Effects of GEM **a** 72 h post-treatment and **b** 96 h post-treatment in BxPC-3 cells. The data is expressed as mean±SEM from three separate experiments in triplicate (n=9). *p<0.05, statistically significant inhibitory effect when compared with gemcitabine solution alone

compounds for the delivery system. In the current study, gemcitabine was solublized in an aqueous matrix prior to emulisification in the chitosan/GMO polymeric matrices. This may create small aqueous pockets with the GMO matrix resulting in an additional diffusional barrier for gemcitabine to partition through. In support of this, we previously reported sustained terminal release profiles for PTX or dexamethasone from chitosan/GMO particles following a significantly reduced burst release compared with gemcitabine in the current study (29). In these previous studies, the burst release was significantly lower and the terminal release rate was higher due to the increased hydrophobicity of paclitaxel and dexamethasone compared with a hydrophilic compound like gemcitabine in the current study. Together, these studies demonstrate the nanostructure composition can alter the surface charge and the release characteristics of the drug. The burst release from the nanostructures in the extracellular media makes the free drug available for transport across the cell membrane through nucleoside transporters expressed on the cellular surfaces. Hence, the total amount of the drug accumulated in the cells is a possible combination of both free drug entering the cells via active transport and from the nanoparticles endocytosed by the cells. These release characteristics may be beneficial in providing both the free drug and the nanostructure-containing drug immediately at the site of action. As discussed earlier, one can expect a higher therapeutic concentration of gemcitabine inside the cell by both transport pathways.

Cellular Association

Gemcitabine, an ionized nucleoside analog, initiates apoptotic cell death through termination of DNA replication and has to be internalized within the nuclear compartment (42). The internalization of most ionized drugs in cells is limited due to the lipophilic nature of the cell membrane thus rendering the intracellular concentrations of the drug very negligible (43). However, gemcitabine is internalized in the cell by a cell membrane bound nucleoside transporter (44–47). Nanostructures significantly increase the intracellular concentration as they are taken up by an energy dependant process like endocytosis (48,49). In addition, the internalization of the nanostructures in the current study appears to be an endo-lysosomal mechanism by the co-localization of green fluorescent dye with the lysotracker red dye. Furthermore, the lack of co-localized green fluorescent dye with the blue fluorescent dye is suggestive that these nanostructures are not localized within the nuclear compartment in these cell types. The mechanisms of nanoparticle internalization are well known and previously discussed (48,49). It has been reported that particles ranging from 300 to 700 nm have a preferred endosomal route for cellular internalization; whereas smaller particles are more suitable for pinocytosis (48–50). The uptake of PLGA nanostructure has been significantly reduced after inhibition of clathrin vesicles but not caveolae (48). The cellular internalization has been suggested to be non-specifically transported through clathrin vesicles (50). This is supported by the fact that coating antisense oligonucleotide loaded PLGA nanostructure with chitosan demonstrated that an increase in both the extent and rate of uptake (51). In the current study, the rapid cellular association of chitosan/GMO nanostructure also suggests that the internalization is actively mediated. The increased cellular accumulation of PTX from this formulation was previously demonstrated in human breast cancer cells MDA-MB-231. In these studies, the increase of cellular accumulation with the paclitaxel nanostructures was 4-fold compared with paclitaxel solution (29). In contrast, the increased accumulation of gemcitabine in the current study was limited to only 2-fold with the nanostructures compared with gemcitabine solution. It would be expected that a transported compound would be internalized within the cell at a

Table II. The *In Vitro* Effects of Gemcitabine in Pancreatic Cancer Models

In vitro cell model post-treatment time with gemcitabine	Nanoparticles mean IC50 (M)	Solution mean IC50 (M)
Mia PaCa-2 cells 72 h post-treatment	$7.52\times10^{-6}\pm2.52\times10^{-6}$	0.055±0.009
Mia PaCa-2 Cells 96 h post-treatment	$4.92\times10^{-6}\pm7.75\times10^{-8}$	0.008±0.0003
BxPC-3 cells 72 h post-treatment	$3.56\times10^{-4}\pm1.21\times10^{-4}$	0.056±0.009
BxPC-3 cells 96 h post-treatment	$5.54\times10^{-6}\pm4.88\times10^{-7}$	0.008±0.0003

The data is expressed as mean from three separate experiments in triplicate (n=9)

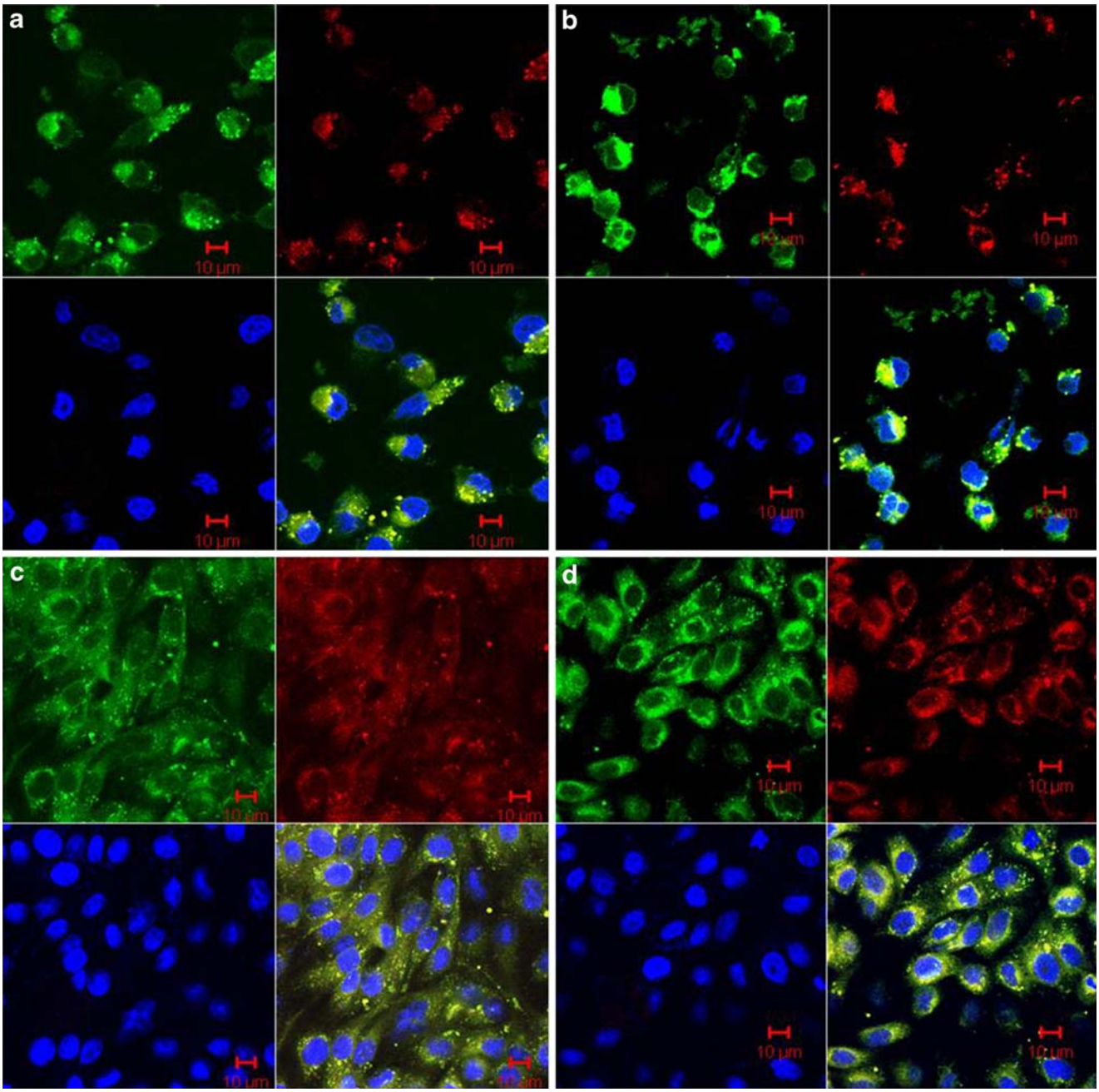

Fig. 6. Cellular accumulation and sub-cellular localization of Fluorescent NPs **a** 30 min and **b** 60 min in Mia PaCa-2 cells or **c** 30 min and **d** 60 min in BxPC-3 cells

higher rate, and thus a reduced difference in cellular accumulation would be observed. The higher accumulation of gemcitabine in BxPC-3 cells compared with Mia PaCa-2 cells can be attributed to the differences in the mucin producing capabilities of the two cell lines. Both, BxPC-3 and Mia PaCa-2 are reported to produce mucin and other glycoproteins owing to an over expression of MUC family genes (33,34). BxPC-3 cell lines are better differentiated and display a higher expression of MUC1, 2, 4, and 5 genes compared with Mia PaCa-2 cells (33). In our previous studies with chitosan/GMO as a delivery vehicle for paclitaxel, the cellular association was found to be dependent on the mucin levels with a higher association in Calu-3 cells than Caco-2 cells (32). The differential levels of cellular accumulation of gemcitabine in the two cell lines are in congruence with our previous findings. The significance of these data demonstrates the bioadhesive and sustained delivery properties of the nanostructures may increase the duration of chemotherapeutic effect of gemcitabine.

CONCLUSION

In conclusion, this formulation generates cationic nanostructures that can be stored in a lyophilized powder that is easily resuspended in an injectable aqueous matrix. In

addition, the mucoadhesive properties of chitosan/GMO nanostructure show evidence of significant increases in cellular accumulation, intracellular internalization and gemcitabine induced cytotoxicity in two pancreatic cancer cell lines. Furthermore, the advantages of gemcitabine incorporated into chitosan/GMO nanostructures may increase the therapeutic window allowing lower doses to be administered.

ACKNOWLEDGEMENTS

These studies were supported in part by a Department of Defense Concept Award BC045664 and Health Future Foundation Grant, Creighton University, Omaha, NE.

REFERENCES

1. Jemal A *et al*. Cancer statistics, 2006. CA Cancer J Clin. 2006;56 (2):106–30.
2. Freelove R, Walling AD. Pancreatic cancer: diagnosis and management. Am Fam Physician. 2006;73(3):485–92.
3. Hertel LW *et al*. Grindey Evaluation of the antitumor activity of gemcitabine (2′, 2′-difluoro-2′-deoxycytidine). Cancer Res. 1990;50(14):4417–22.
4. Plunkett W *et al*. Preclinical characteristics of gemcitabine. Anticancer Drugs. 1995;6 Suppl 6:7–13.
5. Burris HA *et al*. Improvements in survival and clinical benefit with gemcitabine as first-line therapy for patients with advanced pancreas cancer: a randomized trial. J Clin Oncol. 1997;15 (6):2403–13.
6. Heinemann V *et al*. Comparison of the cellular pharmacokinetics and toxicity of 2′, 2′-difluorodeoxycytidine and 1-beta-D-arabinofuranosylcytosine. Cancer Res. 1988;48(14):4024–31.
7. Abbruzzese JL *et al*. A phase I clinical, plasma, and cellular pharmacology study of gemcitabine. J Clin Oncol. 1991;9(3): 491–8.
8. Reid JM *et al*. Phase I trial and pharmacokinetics of gemcitabine in children with advanced solid tumors. J Clin Oncol. 2004;22 (12):2445–51.
9. Moog R *et al*. Change in pharmacokinetic and pharmacodynamic behavior of gemcitabine in human tumor xenografts upon entrapment in vesicular phospholipid gels. Cancer Chemother Pharmacol. 2002;49(5):356–66.
10. Mackey JR *et al*. Functional nucleoside transporters are required for gemcitabine influx and manifestation of toxicity in cancer cell lines. Cancer Res. 1998;58(19):4349–57.
11. Pastor-Anglada M *et al*. Nucleoside transporters in chronic lymphocytic leukaemia. Leukemia. 2004;18(3):385–93.
12. Gourdeau H *et al*. Mechanisms of uptake and resistance to troxacitabine, a novel deoxycytidine nucleoside analogue, in human leukemic and solid tumor cell lines. Cancer Res. 2001;61 (19):7217–24.
13. Yang J *et al*. Magnetic PECA nanoparticles as drug carriers for targeted delivery: synthesis and release characteristics. J Microencapsul. 2006;23(2):203–12.
14. Yang J *et al*. Preparation of poly epsilon-caprolactone nanoparticles containing magnetite for magnetic drug carrier. Int J Pharm. 2006;324(2):185–90.
15. Patra CR *et al*. Targeted delivery of gemcitabine to pancreatic adenocarcinoma using cetuximab as a targeting agent. Cancer Res. 2008;68(6):1970–8.
16. Gang J *et al*. Magnetic poly epsilon-caprolactone nanostructure containing Fe3O4 and gemcitabine enhance anti-tumor effect in pancreatic cancer xenograft mouse model. J Drug Target. 2007;15(6):445–53.
17. Stella B *et al*. Encapsulation of gemcitabine lipophilic derivatives into polycyanoacrylate nanospheres and nanocapsules. Int J Pharm. 2007;344(1–2):71–7.
18. Reddy LH, Couvreur P. Novel approaches to deliver gemcitabine to cancers. Curr Pharm Des. 2008;14(11):1124–37.
19. Huang LS *et al*. Preparation of gemcitabine polybutylcyanoacrylate nanoparticles. Nan Fang Yi Ke Da Xue Xue Bao. 2007;27 (11):1653–6.
20. Galmarini CM *et al*. Polymeric nanogels containing the triphosphate form of cytotoxic nucleoside analogues show antitumor activity against breast and colorectal cancer cell lines. Mol Cancer The. 2008;7(10):3373–80.
21. Arias JL *et al*. Polymeric nanoparticulate system augmented the anticancer therapeutic efficacy of gemcitabine. J Drug Target. 2009;17(8):586–98.
22. Li Y *et al*. Up-regulation of miR-200 and let-7 by natural agents leads to the reversal of epithelial-to-mesenchymal transition in gemcitabine-resistant pancreatic cancer cells. Cancer Res. 2009;69(16):6704–12.
23. Bernkop-Schnurch A *et al*. Thiomers: preparation and *in vitro* evaluation of a mucoadhesive nanoparticulate drug delivery system. Int J Pharm. 2006;317(1):76–81.
24. Zheng F *et al*. Chitosan nanoparticle as gene therapy vector via gastrointestinal mucosa administration: results of an *in vitro* and *in vivo* study. Life Sci. 2007;80(4):388–96.
25. De Campos AM *et al*. Chitosan nanostructure: a new vehicle for the improvement of the delivery of drugs to the ocular surface. Application to cyclosporin A. Int J Pharm. 2001;224 (1–2):159–68.
26. Sandri G *et al*. Nanostructure based on N-trimethylchitosan: evaluation of absorption properties using *in vitro* (Caco-2 cells) and *ex vivo* (excised rat jejunum) models. Eur J Pharm Biopharm. 2007;65(1):68–77.
27. Engstrom S. Drug delivery from cubic and other lipid-water phases. Lipid Technol. 1990;2:42–5.
28. Hyde ST *et al*. A cubic structure consisting of a lipid bilayer forming in infinite periodic minimum surface of the gyriod type in the glycerylmonooleate-water system. Z Krystallogar. 1984;168:213–9.
29. Trickler WJ *et al*. A novel nanoparticle formulation for sustained paclitaxel delivery. AAPS PharmSciTech. 2008;9(2):486–93.
30. Ganguly S, Dash AK. A novel *in situ* gel for sustained drug delivery and targeting. Int J Pharm. 2004;276(1–2):83–92.
31. Trickler WJ. The *in vitro* sub-cellular localization and *in vivo* efficacy of novel Chitosan/GMO nanostructures containing paclitaxel. Pharm Res. 2009;26(8):1963–73.
32. Jauhari S, Dash AK. A mucoadhesive *in situ* gel delivery system for paclitaxel. AAPS PharmSciTech. 2006;7(2):E53.
33. Sipos B *et al*. A comprehensive characterization of pancreatic ductal carcinoma cell lines: towards the establishment of an *in vitro* research platform. Virchows Arch. 2003;442(5):444–52.
34. Yonezawa S *et al*. Differential mucin gene expression in human pancreatic and colon cancer cells. Biochem J. 1991;276(Pt 3):599–605.
35. Takeuchi H *et al*. Novel mucoadhesion tests for polymers and polymer-coated particles to design optimal mucoadhesive drug delivery systems. Adv Drug Deliv Rev. 2005;57(11): 1583–94.
36. Takeuchi H *et al*. Mucoadhesive nanoparticulate systems for peptide drug delivery. Adv Drug Deliv Rev. 2001;47(1):39–54.
37. Takeuchi H *et al*. Mucoadhesion of polymer-coated liposomes to rat intestine *in vitro*. Chem Pharm Bull (Tokyo). 1994;42 (9):1954–6.
38. Takeuchi H *et al*. Enteral absorption of insulin in rats from mucoadhesive chitosan-coated liposomes. Pharm Res. 1996;13 (6):896–901.
39. Howard KA *et al*. RNA interference *in vitro* and *in vivo* using a novel chitosan/siRNA nanoparticle system. Mol Ther. 2006;14 (4):476–84.
40. Shikata F *et al*. *In vitro* cellular accumulation of gadolinium incorporated into chitosan nanostructure designed for neutron-capture therapy of cancer. Eur J Pharm Biopharm. 2002;53 (1):57–63.
41. Takeuchi H *et al*. Effectiveness of submicron-sized, chitosan-coated liposomes in oral administration of peptide drugs. Int J Pharm. 2005;303(1–2):160–70.

42. Achanta G *et al*. Interaction of p53 and DNA-PK in response to nucleoside analogues: potential role as a sensor complex for DNA damage. Cancer Res. 2001;61(24):8723–9.
43. Gerweck LE. Tumor pH: implications for treatment and novel drug design. Semin Radiat Oncol. 1998;8(3):176–82.
44. Burke T *et al*. Interaction of 2′, 2′-difluorodeoxycytidine (gemcitabine) and formycin B with the Na+-dependent and -independent nucleoside transporters of Ehrlich ascites tumor cells. J Pharmacol Exp Ther. 1998;286(3):1333–40.
45. Hammond JR *et al*. [3H]gemcitabine uptake by nucleoside transporters in a human head and neck squamous carcinoma cell line. J Pharmacol Exp Ther. 1999;288(3):1185–91.
46. Bergman AM *et al*. Increased sensitivity to gemcitabine of P-glycoprotein and multidrug resistance-associated protein-over-expressing human cancer cell lines. Br J Cancer. 2003;88 (12):1963–70.
47. Yao J *et al*. The mechanism of resistance to 2′, 2′-difluorodeoxycytidine (gemcitabine) in a pancreatic cancer cell line. Zhonghua Zhong Liu Za Zhi. 2005;27(12):721–6.
48. Rejman J *et al*. Size-dependent internalization of particles via the pathways of clathrin- and caveolae-mediated endocytosis. Biochem J. 2004;377(Pt 1):159–69.
49. Panyam J *et al*. Rapid endo-lysosomal escape of poly(DL-lactide-co-glycolide) nanostructure: implications for drug and gene delivery. Faseb J. 2002;16(10):1217–26.
50. Chavanpatil MD *et al*. Nanostructure for cellular drug delivery: mechanisms and factors influencing delivery. J Nanosci Nanotechnol. 2006;6(9–10):2651–63.
51. Nafee N *et al*. Chitosan-coated PLGA nanostructure for DNA/RNA delivery: effect of the formulation parameters on complexation and transfection of antisense oligonucleotides. Nanomedicine. 2007;3(3):173–83.